

Weak coupling d -wave BCS superconductivity and unpaired electrons in overdoped $\text{La}_{2-x}\text{Sr}_x\text{CuO}_4$ single crystals

Yue Wang, Jing Yan, Lei Shan, and Hai-Hu Wen*

National Laboratory for Superconductivity, Institute of Physics and Beijing National Laboratory for Condensed Matter Physics, Chinese Academy of Sciences, P.O. Box 603, Beijing 100080, People's Republic of China

Yoichi Tanabe, Tadashi Adachi, and Yoji Koike

Department of Applied Physics, Graduate School of Engineering, Tohoku University, 6-6-05 Aoba, Aramaki, Aoba-ku, Sendai 980-8579, Japan

The low-temperature specific heat (SH) of overdoped $\text{La}_{2-x}\text{Sr}_x\text{CuO}_4$ single crystals ($0.178 \leq x \leq 0.290$) has been measured. For the superconducting samples ($0.178 \leq x \leq 0.238$), the derived gap values (without any adjusting parameters) approach closely onto the theoretical prediction $\Delta_0 = 2.14k_B T_c$ for the weak-coupling d -wave BCS superconductivity. In addition, the residual term $\gamma(0)$ of SH at $H = 0$ increases with x dramatically when beyond $x \sim 0.22$, and finally evolves into the value of a complete normal metallic state at higher doping levels, indicating growing amount of unpaired electrons. We argue that this large $\gamma(0)$ cannot be simply attributed to the pair breaking induced by the impurity scattering, instead the phase separation is possible.

PACS numbers: 74.25.Bt, 74.20.Rp, 74.25.Dw, 74.72.Dn

I. INTRODUCTION

For hole-doped cuprates, it is now generally perceived that the superconducting state has robust d -wave symmetry.¹ In the underdoped region, due to the presence of the pseudogap and other possible competing orders,^{2,3} the measured quasiparticle gap may not reflect the real superconducting gap. In contrast, in the overdoped region, the normal state properties can be described reasonably well by the Fermi liquid picture,⁴ although still with electronic correlation to some extent.⁵ Under this circumstance, one may think that the overdoped cuprate provides a clean gateway to the intrinsic high- T_c superconducting state. To accumulate experimentally accessible parameters, such as the superconducting gap, and compare them with the mean field BCS prediction in this very region is thus expected to be particularly valuable.

Another puzzling point in the overdoped cuprates is that the superfluid density ρ_s , determined by muon spin relaxation (μSR) technique decreases just as the transition temperature T_c when beyond a critical doping point $p_c \sim 0.19$.^{6,7,8} This is actually not demanded by the BCS theory. The decrease of ρ_s , first reported in $\text{Ti}_2\text{Ba}_2\text{CuO}_{6+\delta}$ (Ti2201) and subsequently confirmed in other families of cuprates,^{8,9} was attributed to the unpaired carriers at $T \rightarrow 0$ in overdoped cuprates.⁶ Similar conclusion was also drawn from studies of the optical conductivity^{10,11} and magnetization.¹² Recently, the Meissner volume fraction was revealed to decrease as T_c with increasing doping in overdoped $\text{La}_{2-x}\text{Sr}_x\text{CuO}_4$ (LSCO) and the result was suggested to be consistent with the occurrence of a phase separation into superconducting and normal-state regions.¹³ It is thus highly desired to use the specific heat (SH) which is very sensitive to the quasiparticle density of states (DOS) at the Fermi level to directly probe these unpaired charge carriers.

In this paper we shall address these two issues by the low-temperature SH which has established its importance to identify the pairing symmetry in high- T_c cuprates over the past

decade.¹⁴ Recently, the quantitative analysis shows that it provides a bulk way to obtain the magnitude of the superconducting gap.^{15,16} By analyzing the field-induced SH, it is found that the pairing symmetry in the overdoped regime (up to $x = 0.238$) is still d -wave and the derived gap values Δ_0 approach closely onto the theoretical prediction of the weak-coupling d -wave BCS superconductivity. Our data also reveal a quick growing of the residual term $\gamma(0)$ of SH at $T \rightarrow 0$ with increasing doping, which cannot be simply attributed to the pair breaking induced by the impurity scattering.

II. EXPERIMENT

Single crystals of LSCO were grown by the traveling-solvent floating-zone method. Details of the sample preparation have been given elsewhere.^{13,17} The Sr content of the sample, x , taken as the hole concentration p , was determined from the inductively coupled plasma measurement. Figure 1(a) shows the dc magnetization curves measured in 10 Oe after the zero-field cooling (ZFC) mode using a SQUID magnetometer, where the onset of the diamagnetic signal was defined as the critical temperature T_c . Six samples have been measured, with $x = 0.178, 0.202, 0.218, 0.238, 0.259, 0.290$ and $T_c = 36, 30.5, 25, 19.5, 6.5$, and below 1.7 K, respectively. As shown in Fig. 1(b), the T_c can be described well by the empirical formula¹⁸ $T_c/T_c^{\text{max}} = 1 - 82.6(x - 0.16)^2$ with $T_c^{\text{max}} = 38$ K. The SH measurements were performed on an Oxford Maglab cryogenic system using the thermal relaxation technique, as described in detail previously.¹⁹ The temperature was down to 1.9 K and the magnetic field was applied parallel to c -axis in the measurements.

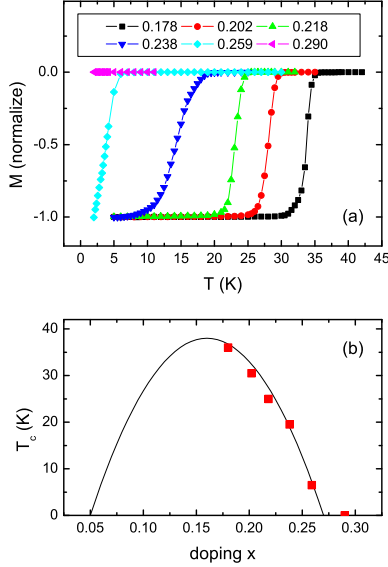


FIG. 1: (color online) (a): Temperature dependence of DC magnetization measured in ZFC mode at 10 Oe. The curves are normalized to unity with the value at the lowest temperatures. (b): Doping dependence of T_c (squares). The empirical formula (see text) is plotted as the solid line.

III. RESULTS AND DISCUSSION

The raw data of SH for all six samples in various H at $T < 7$ K are shown in Fig. 2. To separate the electronic SH from other contributions, the data are fit to $C(T, H) = \gamma T + C_{\text{ph}}T + C_{\text{Sch}}(T, H)$, where $C_{\text{ph}}T = \beta T^3$ is the phonon SH. $C_{\text{Sch}}(T, H)$ is the two-level Schottky anomaly with the form D/T^2 in $H = 0$ and $f x^2 e^x / (1 + e^x)^2$ ($x = g\mu_B H / k_B T$) in $H \neq 0$, where μ_B is the Bohr magneton, g the Landé factor, and f the concentration of spin-1/2 particles. The first linear- T term, γT , contains the electronic SH and resides in the heart of the present study. As demonstrated by the solid lines in Fig. 2(a)-(e), all data sets can be described reasonably well by the above expression. For C_{ph} and the Debye temperature Θ_D the values derived here are in consistent with previous reports on the sample at similar doping level.^{5,20} For C_{Sch} , the yielded f is relatively constant at high fields with an averaged value ~ 3 mJmol⁻¹K⁻¹ for different samples. This low f reflects the small contribution of C_{Sch} to the total SH and assures the reliable determination of γ .

In zero-field, after removing the Schottky term C_{Sch} and by doing a linear extrapolation to the data shown in Fig. 2(f) to $T = 0$ K we can determine the residual term $\gamma(0)$ of SH. By increasing H , an increase in γ is observed for $0.178 \leq x \leq 0.238$, as shown in Fig. 2(a)-(d), corresponding to $\gamma = \gamma(0) + \gamma(H)$ with $\gamma(H)$ the coefficient of the field-induced SH. For d -wave superconductors, it was theoretically pointed out that the $\gamma(H)$ is proportional to \sqrt{H} due to line nodes of the gap,²¹ which has been confirmed in several

experiments.^{14,19} Figure 3 summarizes the field dependence of the $\gamma(H)$ for the overdoped LSCO. It is clear that for all four samples, the $\gamma(H)$ is well described by $A\sqrt{H}$ with A a doping-dependent constant, as exemplified by the solid lines in Fig. 3. This indicates that in overdoped LSCO the gap remains robust d -wave symmetry.

Next one can further obtain the gap magnitude by investigating $\gamma(H)$ quantitatively. Fundamentally, $\gamma(H)$ arises from the Doppler shift of the quasiparticle spectrum near the nodes due to the supercurrent flowing around vortices and thus directly relates to the slope of the gap at the node, $v_\Delta = 2\Delta_0/\hbar k_F$ with Δ_0 the d -wave maximum gap in the gap function $\Delta = \Delta_0 \cos(2\phi)$, k_F the Fermi vector near nodes (taking $\sim 0.7 \text{ \AA}^{-1}$ as obtained from ARPES²²). Explicitly, the relation between v_Δ and the prefactor A is given by

$$A = \frac{4k_B^2}{3\hbar} \sqrt{\frac{\pi}{\Phi_0}} \frac{nV_{\text{mol}}}{d} \frac{a}{v_\Delta} \quad (1)$$

where Φ_0 is the flux quantum, n the number of CuO₂ planes per unit cell, d the c -axis lattice constant, V_{mol} the volume per mole, and $a = 0.465$ for a triangular vortex lattice.^{23,24} Inset of Fig. 3 shows the doping dependence of A by fitting the data to $\gamma(H) = A\sqrt{H}$. Thus, with the known parameters for LSCO ($n = 2$, $d = 13.28 \text{ \AA}$, $V_{\text{mol}} = 58 \text{ cm}^3$), the doping dependence of v_Δ and Δ_0 can be derived without any adjusting parameters according to Eq. (1). In this way we extracted the gap values $\Delta_0 = 9.2 \pm 0.7$, 6.6 ± 0.3 and 5.6 ± 0.3 meV for $x = 0.178$, 0.202 and 0.218 , respectively (for $x = 0.238$, the observed A should be corrected due to the volume correction which will be addressed later). It can be seen immediately that Δ_0 decreases with increasing doping in the overdoped LSCO, concomitant with the decrease of T_c . The same trend of T_c and Δ_0 with overdoping implies that the suppression of superconductivity mainly comes from the decrease in the pairing gap. Figure 4 plots the doping dependence of Δ_0 , together with the value extracted from SH in underdoped and optimal doped LSCO single crystals.^{16,25} For comparison, the weak-coupling d -wave BCS gap relation $\Delta_0 = 2.14k_B T_c$ is also plotted as a dotted curve in Fig. 4(a) and a dotted horizontal line in Fig. 4(b),²⁶ where T_c is determined by the empirical formula described before. Remarkably, beyond $x \sim 0.19$, the experimental data approaches closely onto the theoretical prediction, revealing a strong evidence for the weak coupling d -wave BCS superconductivity. Previous results about Δ_0 determined by scanning tunnelling spectroscopy²⁷ and penetration depth measurements²⁸ are in excellent quantitative agreement with our present results, which strongly supports the validity of the present analysis.

Now we examine the implication of the residual term $\gamma(0)$ in zero-field. Figure 5(a) summarizes the doping dependence of $\gamma(0)$, where the values from previous studies are also included.^{19,25} For comparison, the normal-state SH coefficient γ_N in the corresponding doping region is shown together.²⁹ We can see that the $\gamma(0)$ increases with doping up to $x = 0.259$. For the nonsuperconducting $x = 0.290$ sample, the $\gamma(0)$ is actually the γ_N , which shows good consistency with the previous value. Note that for $x = 0.259$, the $\gamma(0)$ is already close to the reported γ_N . Close to the optimal doping point

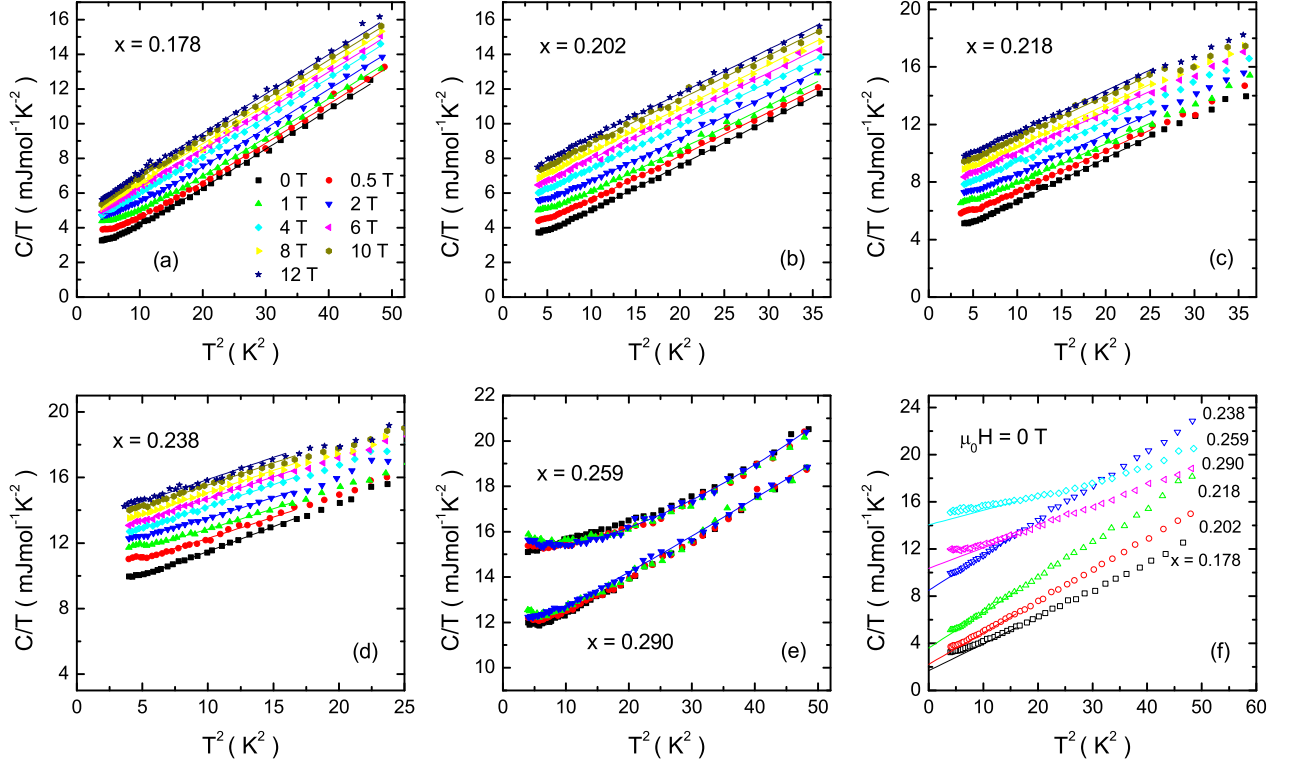


FIG. 2: (color online) Temperature and magnetic field dependence of SH in C/T vs T^2 plot. (a)-(e): Raw data for all six samples (symbols). $\mu_0 H$ varies up to 12 T for $0.178 \leq x \leq 0.238$ while up to 2 T for $x = 0.259$ and 0.290 . The solid lines represent the theoretical fit (see text). The fits are limited to $T = 7, 6, 5,$ and 4 K for $x = 0.178, 0.202, 0.218,$ and 0.238 , respectively. For $x = 0.259$ and 0.290 , the fits are ranged to 7 K. (f): Replot the data at $\mu_0 H = 0$ T for all samples (symbol: $\square = 0.178, \circ = 0.202, \triangle = 0.218, \nabla = 0.238, \diamond = 0.259, \blacktriangleleft = 0.290$). The dotted lines are extrapolations of the data down to $T = 0$ K with the Schottky anomaly subtracted.

the small $\gamma(0)$ may be attributed to the impurity scattering by which a finite DOS is generated for a d -wave superconductor. However the large $\gamma(0)$ appearing beyond $x \sim 0.22$ cannot be simply attributed to this reason. This can be understood by having an estimation on the impurity scattering induced DOS $\gamma_{\text{res}}^{\text{imp}}$ in the superconducting state, which has the relation $\gamma_{\text{res}}^{\text{imp}}/\gamma_N = (2\gamma_0/\pi\Delta_0) \ln(\Delta_0/\gamma_0)$ with γ_0 the pair breaking parameter.³⁰ Also in the unitarity limit, $\gamma_0 \approx 0.6\sqrt{\Gamma\Delta_0}$ with $\Gamma = 1/2\tau_0$ the normal state quasiparticle scattering rate which can be estimated from the residual resistivity $\rho_0 = m^*/ne^2\tau_0$ and the plasma frequency $\omega_p = \sqrt{ne^2/\epsilon_0 m^*}$. With $\rho_0 = 26 \mu\Omega\text{cm}$ and $\omega_p \approx 1.2$ eV for $x = 0.238$,³¹ one gets $\hbar\Gamma \approx 2.5$ meV. Assuming $\Delta_0 = 2.14k_B T_c$, we obtain $\gamma_{\text{res}}^{\text{imp}}/\gamma_N \approx 0.2$ and therefore $\gamma_{\text{res}}^{\text{imp}} \approx 2.9 \text{ mJmol}^{-1}\text{K}^{-2}$ for $x = 0.238$, which is far below the $\gamma(0)$.

Furthermore, if the large $\gamma(0)$ is completely induced by the impurity scattering, the field-induced $\gamma(H)$ at low H is expected to deviate from the \sqrt{H} dependence and instead show an $H \ln H$ behavior: $\gamma(H) \approx \Lambda(H/H_{c2}) \ln[B(H_{c2}/H)]$, where

$\Lambda = \Delta_0 a^2 \gamma_N / 8\gamma_0$ with $B = \pi/2a^2$.³² In Fig. 6 we present the fits to $\gamma(H)$ for $H \leq 4$ T with this function. First, we leave Λ and H_{c2} as both free fitting parameters (fit1) and the best fit is shown in Fig. 6(a). As shown in Fig. 6(b), this yields the parameter $\mu_0 H_{c2} < 4$ T for all samples $0.178 \leq x \leq 0.238$. The rather low H_{c2} is physically unacceptable. At the same time, from the parameter Λ , the coefficient of the residual specific heat $\gamma_{\text{res}}^{\text{imp}}$ can be calculated using the expressions and the γ_N described above. It can be seen, for $x \geq 0.218$, the obtained $\gamma_{\text{res}}^{\text{imp}}$ is also inconsistent with the experiment. Secondly, we try to fit the data with H_{c2} fixed within the values shown in the shaded region in Fig. 6(e) (fit2). The transport and Nernst effect measurements have indicated that $\mu_0 H_{c2} \sim 1.5T_c$ (H_{c2} in Tesla and T_c in Kelvin) for the overdoped LSCO.^{33,34} The current SH suggests $\mu_0 H_{c2} > 12$ T for all samples. Hence, in Fig. 6(e) the lower limit of the shaded region is set to be $\mu_0 H_{c2} = 12$ T and the upper limit to be $\mu_0 H_{c2} = 2T_c$. In this case, we could not obtain a satisfactory fit to the data, as indicated by the typical result shown in Fig. 6(d). Again, the

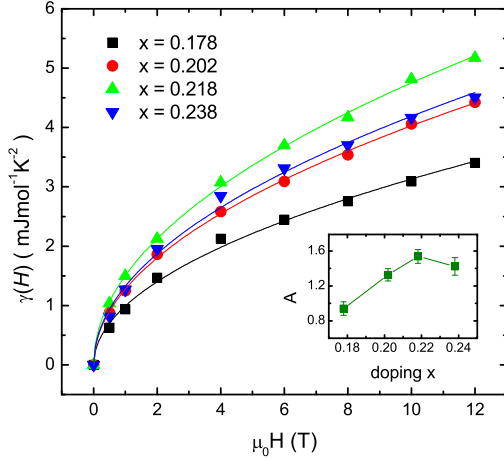


FIG. 3: (color online) Coefficient of the field-induced linear- T specific heat for $0.178 \leq x \leq 0.238$, $\gamma(H) = \gamma - \gamma(0)$ at $T = 0$ K (symbols). The solid lines are the fits to $\gamma(H) = A\sqrt{H}$. Inset: Doping dependence of the prefactor A ($\text{mJmol}^{-1}\text{K}^{-2}\text{T}^{-0.5}$).

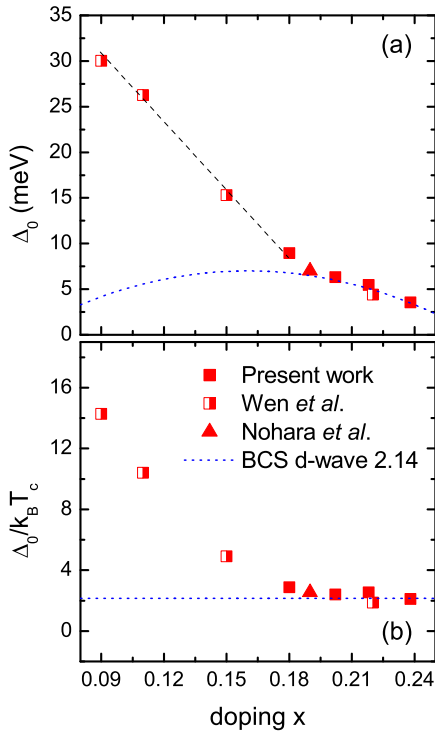


FIG. 4: (color online) Doping dependence of the superconducting gap Δ_0 obtained from SH measurements. (a): Δ_0 vs x . The dashed line is a guide to the eye. (b): $\Delta_0/k_B T_c$ vs x . The values from Ref. 16 (half-filled squares) and Ref. 25 (triangle) are also included. The weak-coupling d-wave BCS value, $\Delta_0 = 2.14k_B T_c$ ($\Delta_0/k_B T_c = 2.14$) is plotted as a dotted curve (horizontal line) in (a) (b). For $x \geq 0.19$, the experiments are consistent with the BCS prediction.

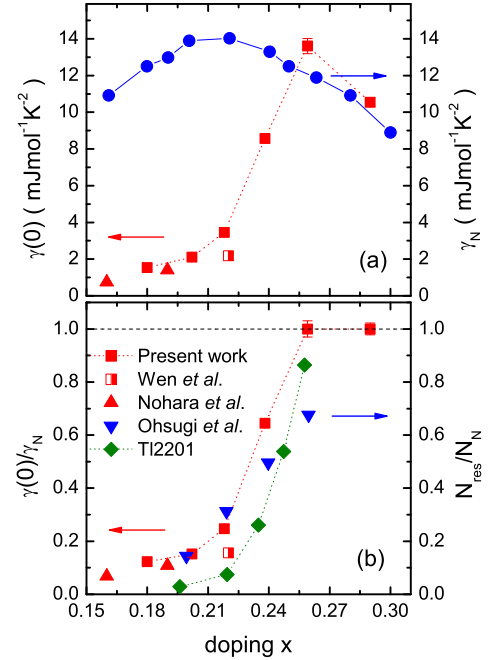


FIG. 5: (color online) (a): Doping dependence of the $\gamma(0)$ in zero field (filled squares) and the normal state SH coefficient, γ_N (circles). The $\gamma(0)$ from Ref. 19 (half-filled square) and Ref. 25 (up-triangles) are also shown. The γ_N is quoted from Ref. 29. (b): Doping dependence of the $\gamma(0)$ in (a) normalized by γ_N , $\gamma(0)/\gamma_N$. The same for TI-2201 (diamonds) is quoted from Ref. 36. The normalized residual spin Knight shift in LSCO,³⁵ N_{res}/N_N , is also shown for comparison (down-triangles).

obtained $\gamma_{\text{res}}^{\text{imp}}$ is contradictory to the measurement (Note, for a given sample, one would obtain the lower $\gamma_{\text{res}}^{\text{imp}}$ with a higher H_{c2}) (Fig. 6(f)). Therefore, it seems that the impurity scattering effect could not account for the field dependence of the $\gamma(H)$.

The above analysis suggests that in highly doped LSCO the $\gamma(0)$ mainly comes from contributions other than the impurity scattering. We attribute it to the presence of nonsuperconducting metallic regions. This can be corroborated by simultaneously having a good consistency with the Volovik's relation $\gamma(H) = A\sqrt{H}$ and the very large ratio $\gamma(0)/\gamma_N$ on the single sample $x = 0.238$. Figure 5(b) shows the ratio of $\gamma(0)/\gamma_N$ together with the normalized residual spin Knight shift,³⁵ N_{res}/N_N , another probe of the residual DOS in the superconducting state. In overdoped TI2201 the low-temperature SH has been measured by Loram *et al.*³⁶ and the $\gamma(5\text{K})/\gamma_N$ is plotted together. We can see that all these quantities show a rapid increase with overdoping, indicating a generic property. Actually in LSCO previous results also showed the rapid increase of $\gamma(0)$ with doping in highly overdoped region although those experiments were done on polycrystalline samples.^{29,36} One may argue, in LSCO, that there is a high-temperature tetragonal to orthorhombic structural transition near $x \approx 0.2$,³⁷ which

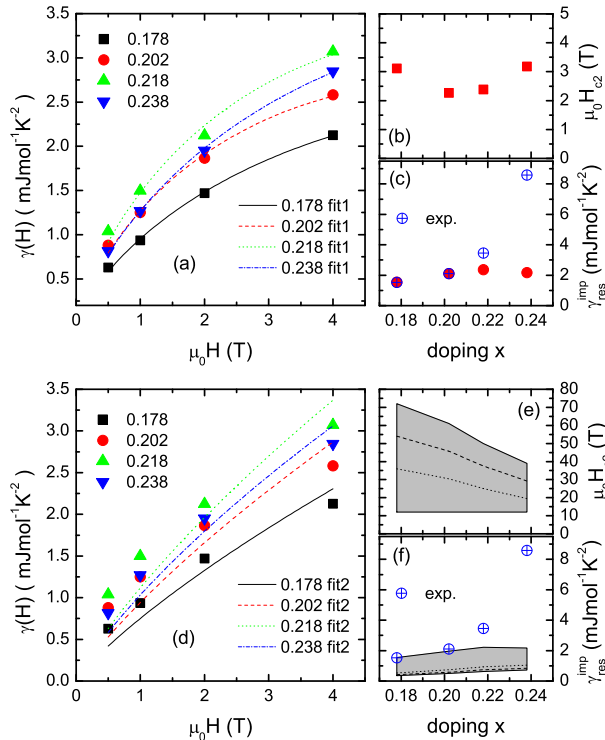


FIG. 6: (color online) Fit low field $\gamma(H)$ to the $H \ln H$ function (see text). (a): Fit1 with Λ and H_{c2} as both free fitting parameters. The yielded parameters (Λ translating to γ_{res}^{imp}) are shown in (b) and (c). (d): Fit2 with H_{c2} fixed within the values shown in the shaded region in (e). The dotted and dashed lines in (e) denote $H_{c2} = 1T_c$ and $1.5T_c$, respectively. The yielded parameter γ_{res}^{imp} is shown in (f) as the shaded region. For comparison, the experimental $\gamma(0)$ is shown in (c) and (f) (circles).

may induce the rapid increase of $\gamma(0)$. We note that, however, in Pr-doped LSCO,³⁸ this subtle structural transition can be tuned to much higher doping level, but the superconducting dome remains unchanged, indicating that the hole concentration rather than the slight structure distortion plays a dominant role here. Furthermore, as shown in Fig. 5, a very similar residual $\gamma(0)$ appears in Tl2201, a system without such a structural transition.

The presence of nonsuperconducting metallic phase implies immediately a decrease of the superconducting volume fraction. This can just explain the field dependence of the SH in $x = 0.238$ and 0.259 samples. For $x = 0.238$, the observed A is even lower than that for $x = 0.218$, implying a significantly reduced superconducting volume fraction. Taking this into account, the A used to derive the Δ_0 for this sample, should be corrected roughly as $A\gamma_N/[\gamma_N - \gamma(0)]$, with the assumption that the volume ratio is similar to the DOS ratio. The gap value yielded with this correction is about 3.5 meV, which also

scales with T_c in d -wave BCS manner and is plotted in Fig. 4. For $x = 0.259$, the sample shows a large $\gamma(0)$ being close to the γ_N , indicating a rather small superconducting volume fraction.

So far, we have shown that in overdoped LSCO, the superconducting gap decreases with increasing x and at high doping levels, there exist nonsuperconducting metallic regions at $T \rightarrow 0$. Let us discuss the implications of both effects. Previously it was suggested that the suppression of T_c in overdoped regime may come from the increasing pair breaking effect. Our present result, however, does not support this proposal since T_c is found to scale with Δ_0 in good agreement with d -wave BCS theory, which implies that the decrease in T_c should originate from an underlying reduction in the pairing strength. This point may also be helpful to elucidate the origin of the presence of nonsuperconducting metallic regions in the overdoped sample, which is yet unclear. Currently several scenarios have been proposed to account for this anomalous phenomenon. One is that the overdoped cuprate may spontaneously phase separate into the hole-poor superconducting region and the hole-rich normal Fermi liquid region due to the competition in energy between these two phases.³⁹ Another scenario is associated with the microscopic hole doping state.¹³ It was speculated that in the overdoped regime the holes were doped directly into the Cu3d orbital rather O2p,⁴⁰ which is expected to produce free Cu spins and/or disturb the antiferromagnetic correlation between Cu spins. Around these holes, the superconductivity is destroyed, forming the normal state region. Our present result seems supporting this scenario with the assumption that the superconductivity is magnetic in origin and the suppression of Δ_0 originates from the disturbing of the antiferromagnetic correlation with overdoping.

IV. SUMMARY

In summary, low-temperature SH in overdoped LSCO single crystals has revealed two interesting findings: (1) The field-induced SH follows the prediction of d -wave symmetry yielding a gap value Δ_0 approaching closely onto the weak-coupling d -wave BCS relation $\Delta_0 = 2.14k_B T_c$; (2) At high doping levels, the residual SH term $\gamma(0)$ rises dramatically with doping, which suggests the existence of unpaired electrons possible in association with the normal metallic regions. These discoveries may carry out a common feature in cuprate superconductors and give important clues to the high- T_c pairing mechanism.

Acknowledgments

This work is supported by the National Science Foundation of China, the Ministry of Science and Technology of China (973 project No: 2006CB601000, 2006CB921802), and Chinese Academy of Sciences (Project ITSNEM).

- * Electronic address: hhwen@aphy.iphy.ac.cn
- ¹ C. C. Tsuei, J. R. Kirtley, G. Hammerl, J. Mannhart, H. Raffy, and Z. Z. Li, *Phys. Rev. Lett.* **93**, 187004 (2004).
 - ² J. Orenstein and A. J. Millis, *Science* **288**, 468 (2000).
 - ³ D. A. Bonn, *Nature Phys. (London)* **2**, 159 (2006).
 - ⁴ C. Proust, E. Boaknin, R. W. Hill, L. Taillefer, and A. P. Mackenzie, *Phys. Rev. Lett.* **89**, 147003 (2002).
 - ⁵ S. Nakamae, K. Behnia¹, N. Mangkorntong, M. Nohara, H. Takagi, S. J. C. Yates, and N. E. Hussey, *Phys. Rev. B* **68**, R100502 (2003).
 - ⁶ Y. J. Uemura, A. Keren, L. P. Le, G. M. Luke, W. D. Wu, Y. Kubo, T. Manako, Y. Shimakawa, M. Subramanian, J. L. Cobb, and J. T. Markert, *Nature (London)* **364**, 605 (1993).
 - ⁷ Ch. Niedermayer, C. Bernhard, U. Binninger, H. Glöckler, J. L. Tallon, E. J. Ansaldo, and J. I. Budnick, *Phys. Rev. Lett.* **71**, 1764 (1993).
 - ⁸ C. Bernhard, J. L. Tallon, Th. Blasius, A. Golnik, and Ch. Niedermayer, *Phys. Rev. Lett.* **86**, 1614 (2001).
 - ⁹ J.-P. Locquet, Y. Jaccard, A. Cretton, E. J. Williams, F. Arrouy, E. Mächler, T. Schneider, Ø. Fischer, and P. Martinoli, *Phys. Rev. B* **54**, 7481 (1996).
 - ¹⁰ J. Schützmann, S. Tajima, S. Miyamoto, and S. Tanaka, *Phys. Rev. Lett.* **73**, 174 (1994).
 - ¹¹ S. Uchida, K. Tamasaku, and S. Tajima, *Phys. Rev. B* **53**, 14558 (1996).
 - ¹² H. H. Wen, X. H. Chen, W. L. Yang, and Z. X. Zhao, *Phys. Rev. Lett.* **85**, 2805 (2000).
 - ¹³ Y. Tanabe, T. Adachi, T. Noji, and Y. Koike, *J. Phys. Soc. Jpn.* **74**, 2893 (2005).
 - ¹⁴ N. E. Hussey, *Adv. Phys.* **51**, 1685 (2002).
 - ¹⁵ Y. Wang, B. Revaz, A. Erb, and A. Junod, *Phys. Rev. B* **63**, 094508 (2001).
 - ¹⁶ H. H. Wen, L. Shan, X. G. Wen, Y. Wang, H. Gao, Z. Y. Liu, F. Zhou, J. W. Xiong, and W. X. Ti, *Phys. Rev. B* **72**, 134507 (2005).
 - ¹⁷ T. Adachi, Y. Tanabe, T. Noji, H. Sato, and Y. Koike, *Physica C* **445-448**, 14 (2006).
 - ¹⁸ J. L. Tallon, C. Bernhard, H. Shaked, R. L. Hitterman, and J. D. Jorgensen, *Phys. Rev. B* **51**, R12911 (1995).
 - ¹⁹ H. H. Wen, Z. Y. Liu, F. Zhou, J. W. Xiong, W. X. Ti, T. Xiang, S. Komiya, X. F. Sun, and Y. Ando, *Phys. Rev. B* **70**, 214505 (2004).
 - ²⁰ S. J. Chen, C. F. Chang, H. L. Tsay, H. D. Yang, and J.-Y. Lin, *Phys. Rev. B* **58**, R14753 (1998).
 - ²¹ G. E. Volovik, *JETP Lett.* **58**, 469 (1993).
 - ²² T. Yoshida, X. J. Zhou, K. Tanaka, W. L. Yang, Z. Hussain, Z.-X. Shen, A. Fujimori, S. Sahrakorpi, M. Lindroos, R. S. Markiewicz, A. Bansil, S. Komiya, Y. Ando, H. Eisaki, T. Kakeshita, and S. Uchida, *Phys. Rev. B* **74**, 224510 (2006).
 - ²³ M. Chiao, R. W. Hill, C. Lupien, L. Taillefer, P. Lambert, R. Gagnon, and P. Fournier, *Phys. Rev. B* **62**, 3554 (2000).
 - ²⁴ I. Vekhter, P. J. Hirschfeld, and E. J. Nicol, *Phys. Rev. B* **64**, 064513 (2001).
 - ²⁵ M. Nohara, H. Suzuki, M. Isshiki, N. Mangkorntong, F. Sakai, and H. Takagi, *J. Phys. Soc. Jpn.* **69**, 1602 (2000).
 - ²⁶ H. Won and K. Maki, *Phys. Rev. B* **49**, 1397 (1994).
 - ²⁷ T. Nakano, N. Momono, M. Oda, and M. Ido, *J. Phys. Soc. Jpn.* **67**, 2622 (1998).
 - ²⁸ C. Panagopoulos and T. Xiang, *Phys. Rev. Lett.* **81**, 2336 (1998).
 - ²⁹ N. Momono, M. Ido, T. Nakano, M. Oda, Y. Okajima, and K. Yamaya, *Physica C* **233**, 395 (1994).
 - ³⁰ G. Preosti, H. Kim, and P. Muzikar, *Phys. Rev. B* **50**, 1259 (1994).
 - ³¹ M. Suzuki, in *Strong Correlation and Superconductivity*, edited by H. Fukuyama *et al.*, (Springler-Verlag, Berlin, 1989).
 - ³² C. Kübert and P. J. Hirschfeld, *Solid State Commun.* **105**, 459 (1998).
 - ³³ Y. Ando, G. S. Boebinger, A. Passner, L. F. Schneemeyer, T. Kimura, M. Okuya, S. Watauchi, J. Shimoyama, K. Kishio, K. Tamasaku, N. Ichikawa, and S. Uchida, *Phys. Rev. B* **60**, 12475 (1999).
 - ³⁴ Y. Wang, L. Li, and N. P. Ong, *Phys. Rev. B* **73**, 024510 (2006).
 - ³⁵ S. Ohsugi, Y. Kitaoka, and K. Asayama, *Physica C* **282-287**, 1373 (1997).
 - ³⁶ J. W. Loram, K. A. Mirza, J. M. Wade, J. R. Cooper, and W. Y. Liang, *Physica C* **235-240**, 134 (1994).
 - ³⁷ H. Takagi, R. J. Cava, M. Marezio, B. Batlogg, J. J. Krajewski, W. F. Peck, Jr., P. Bordet, and D. E. Cox, *Phys. Rev. Lett.* **68**, 3777 (1992).
 - ³⁸ W. Schäfer, M. Breuer, G. Bauer, A. Freimuth, N. Knauf, B. Roden, W. Schlabit, and B. Büchner, *Phys. Rev. B* **49**, R9248 (1994).
 - ³⁹ Y. J. Uemura, *Solid State Commun.* **126**, 23 (2003).
 - ⁴⁰ S. Wakimoto, R. J. Birgeneau, A. Kagedan, H. Kim, I. Swainson, K. Yamada, and H. Zhang, *Phys. Rev. B* **72**, 064521 (2005).